# Essential Roles of Raf/Extracellular Signal-regulated Kinase/Mitogen-activated Protein Kinase Pathway, YY1, and Ca$^{2+}$ Influx in Growth Arrest of Human Vascular Smooth Muscle Cells by Bilirubin*

**Marlon Stoeckius**[‡1], **Anna Erat**[‡§1], **Tatsuya Fujikawa**[‡], **Makoto Hiromura**[‡¶], **Anna Koulova**[‡], **Leo Otterbein**[∥], **Cesario Bianchi**[**], **Edda Tobiasch**[‡‡], **Yossi Dagon**[‡2], **Frank W. Sellke**[**2], and **Anny Usheva**[‡2,3]

*From the* ‡*Medicine, Endocrinology and* ∥*Surgery, Beth Israel Deaconess Medical Center, Harvard Medical School, Boston, Massachusetts 02215, the* **Division of Cardiothoracic Surgery, Alpert Medical School of Brown University Providence, Rhode Island 02912, the* ¶*Multiple Molecular Imaging Research Laboratory, RIKEN Kobe Institute, Hyogo 650-0047, Japan, the* ‡‡*Bonn-Rhein-Sieg University of Applied Sciences, Genetic Engineering and Cell Culture, D-53359 Rheinbach, Germany, and* §*University Hospital Zurich, Clinic for Internal Medicine, 8091 Zurich, Switzerland*

**Background:** Bilirubin circulates throughout the human cardiovascular system. Its interaction with the vascular wall is not well known.

**Results:** Bilirubin alters Raf/ERK/MAPK pathway, cellular transcription factor YY1 location, and calcium-dependent YY1 proteolysis in human vascular cells.

**Conclusion:** At high physiological levels bilirubin, inhibits cell growth, inhibits proliferation, and does not cause apoptosis.

**Significance:** The observations provide opportunities for prevention and treatment of cardiovascular diseases.

The biological effects of bilirubin, still poorly understood, are concentration-dependent ranging from cell protection to toxicity. Here we present data that at high nontoxic physiological concentrations, bilirubin inhibits growth of proliferating human coronary artery smooth muscle cells by three events. It impairs the activation of Raf/ERK/MAPK pathway and the cellular Raf and cyclin D1 content that results in retinoblastoma protein hypophosphorylation on amino acids S608 and S780. These events impede the release of YY1 to the nuclei and its availability to regulate the expression of genes and to support cellular proliferation. Moreover, altered calcium influx and calpain II protease activation leads to proteolytical degradation of transcription factor YY1. We conclude that in the serum-stimulated human vascular smooth muscle primary cell cultures, bilirubin favors growth arrest, and we propose that this activity is regulated by its interaction with the Raf/ERK/MAPK pathway, effect on cyclin D1 and Raf content, altered retinoblastoma protein profile of hypophosphorylation, calcium influx, and YY1 proteolysis. We propose that these activities together culminate in diminished 5 S and 45 S ribosomal RNA synthesis and cell growth arrest. The observations provide important mechanistic insight into the molecular mechanisms underlying the transition of human vascular smooth muscle cells from proliferative to contractile phenotype and the role of bilirubin in this transition.

Early studies established that mitochondria might be a major target of bilirubin, leading to uncoupling of oxidative phosphorylation (1). Other studies indicate that bilirubin could inhibit DNA and protein synthesis in some tissues, as well as cell lines, and induce apoptosis (2, 3).

Apart from its toxic effect at high concentrations, bilirubin also seems to play an important role in protecting cells from oxidative damage by acting as a scavenger of peroxyl, hydroperoxyl, and hydroxyl radicals (4). The extended system of conjugated bilirubin double bonds and the presence of a reactive hydrogen atom underlie its functions as a powerful biological chain-breaking antioxidant, supporting the idea of a beneficial role (4). Indeed, recent clinical data associate the increased total serum bilirubin level with lessened susceptibility to peripheral arterial disease (5) and coronary artery disease (6). Moreover, there is also accumulating evidence from epidemiological studies showing that individuals with high normal plasma bilirubin levels, including individuals with Gilbert syndrome, have a lesser incidence of coronary artery disease and carotid vascular plaque formation (7). Thus, there is considerable clinical evidence that an elevated serum bilirubin level is associated with a diminished susceptibility to atherosclerotic vascular disease. Studies in rats demonstrate a salutary bilirubin effect through its suppression of vascular neointimal formation in the carotid artery because of impaired activation of MAPKs. Involvement of transcription factor YY1 and the retinoblas-

[1] These authors contributed equally to this work.
[2] Joint senior authors.
[3] To whom correspondence should be addressed: Department of Medicine, Endocrinology, Beth Israel Deaconess Medical Center, Harvard Medical School, 3 Blackfan Circle CLS 701, Boston, MA 02215. Tel.: 617 635 3311; Fax: 617 735 3324; E-mail: ausheva@bidmc.harvard.edu.

toma protein (Rb)[4] in rodents has also been proposed. However, an exact molecular mechanism of bilirubin action on human VSMC remains to be established.

Thus, we set out to investigate the mechanisms underlying bilirubin action in primary cell cultures of human coronary artery smooth muscle cells. By treating growth-stimulated primary cell culture with physiologically relevant concentrations of bilirubin in a complex with FBS, we were able to detect an effect of bilirubin on the Raf/MEK/ERK pathway. We report for specific effect on cyclin D1 content and the Rb profile of amino acids phosphorylation. Altered influx of calcium, resulting in calpain II protease circuit activation occurs as well. This culminates in protein cleavage of the transcription factor YY1 by calpain II. Furthermore, we observed alterations in the YY1-regulated expression of 5 S ribosomal RNA (rRNA) and 45 S rRNA. We suggest that this, together with the proteolitically lowered YY1 levels, altered Raf/MEK/ERK pathway, cyclin D1 content, and Rb profile of hypophosphorylation, could explain the growth arrest effect of bilirubin on hVSMC. These observations provide new insights into the molecular mechanisms and pathways underlying the switch of hVSMC from proliferative to contractile phenotype and the role of bilirubin in this transition. These novel observations may provide opportunities for prevention and treatment of cardiovascular diseases by providing the basis for the development of novel therapeutic strategies that target these pathways.

## EXPERIMENTAL PROCEDURES

*Cell Culture, Treatment, and Immunofluorescence*—Human coronary artery smooth muscle cells (hCASMC) from different donors, a female Caucasian 46 years old, a male Caucasian 21 years old, and a male Caucasian 49 years old, from Cambrex were cultivated in SmGM-2 (Cambrex) at 37 °C in a humidified atmosphere of 5% $CO_2$. All of the experiments were performed at passages 5–8 of the cells under continuous subconfluent conditions. For bilirubin treatment, the cells were cultivated up to 70% confluence. The cells were first starved for 12 h in medium with 0.5% FBS and for another 24 h in the absence of FBS. After starvation, the cells were cultivated in medium with 10% FBS and with or without 100 $\mu$M bilirubin. The bilirubin stock solution was prepared in 20 $\mu$M NaOH and 10 mg/ml BSA. The cells were harvested for RNA and protein after 0 h (starved cells), 8, 16, and 24 h upon cultivation with or without bilirubin. In some experiments, 0.5 mM EGTA-AM (Molecular Probes) or 1 mM EGTA were added to the cell medium 20 min prior to harvesting. The intracellular calcium content was compared by treating the cells with 100 nM of fura red for 20 min as recommended by the supplier (Molecular Probes). Fluorescent microscopy (Zeiss Axiovert 135 fluorescence microscope) images of fura red fluorescence at 514-nm excitation and 550-nm emission were collected, and the staining intensity was measured in pixels with ImageJ software (National Institutes of Health) and Adobe PhotoShop. Cell cul-

ture without bilirubin served as a negative control. Measurements were performed in triplicate. The cells were prepared for immunofluorescent microscopy as previously described (8).

*Isolation of RNA and RT-qPCR*—Total RNA is isolated from the cells with the RNeasy Mini kit from (Qiagen) as recommended by the manufacturer. For RT-qPCR experiments, 600 ng of total RNA was reverse transcribed using a cDNA synthesis kit (Invitrogen) with random oligonucleotide primers. For cellular RT-qPCR, 500 ng of total RNA was reverse transcribed using the same conditions as above; 1/10 dilutions were used in triplicate with 0.2 $\mu$M gene-specific primers and 5 $\mu$l of Light-Cycler 480 SYBR Green I Master kit (Stratagene) in 20-$\mu$l reactions. Gene-specific primers were selected (PRIMER BLAST, National Institutes of Health), synthesized, and gel-purified. The sequences of the primers are: 5 S RNA, CCT CCA GTG GTT GTC GAC TT (forward) and GAA CGA CAC ACC ACC GTT C (reverse); 45 S RNA, CCT CCA GTG GTT GTC GAC TT (forward) and GAA CGA CAC ACC ACC GTT C (reverse); $\beta$-actin, AAC TGG AAC GGT GAA GGT GAC AGC (forward) and TGG CTT TTA GGA TGG CAA GGG ACT (reverse); and $\alpha$-smooth muscle actin, AAT GAG ATG GCC ACT GCC GC (forward) and CAG AGT ATT TGC GCT CCG GA (reverse). The relative level of gene expression was normalized to the $\beta$-actin gene.

*[³H]Thymidine Incorporation, Apoptosis, and Cell Cycle Analyses*—For thymidine incorporation, hCASMC were cultivated in 24-well plates. 1 $\mu$Ci of [methyl-³H]thymidine (PerkinElmer Life Sciences) was added per well to measure *de novo* DNA synthesis by determining the level of cellular [³H]thymidine incorporation.

The results of the individual treatments were obtained in duplicate using a scintillation counter (Beckmann). FITC-labeled annexin V (PromoKine) was used to identify early apoptotic cells following the protocol of the supplier. The number of annexin V-positive cells was counted by fluorescence microscopy in four independent experiments. Cell cycle analysis was performed as previously reported (9). DNA content analysis of samples was performed in duplicate using a FACS scan (Becton Dickinson) and analyzed with Cellquest software (Becton Dickinson).

*Protein Isolation and Western Blots*—Total cell lysates were prepared by resuspending the cells in radioimmune precipitation assay buffer (Boston Bioproducts) supplemented with 1 mM EDTA. Nuclear and cytosolic extracts were prepared with the NE-PER kit (Thermo Scientific) following the manufacturer's protocol. The protein concentration of the extracts was determined using the DC protein assay (Bio-Rad) according to the manufacturer's protocol with a BSA standard curve. Routinely 40 $\mu$g of protein/lane was used for Western blot with mouse anti-YY1 antibody (Santa Cruz), chicken polyclonal anti-YY1 antibody (Cell Code, MA), anti-Sp1 antibody (Santa Cruz), the antibodies to total Rb, hypophosphorylated Rb (D20), phospho-Rb (S608), phospho-Rb (S612), pPhospho-Rb (S780), ERK (p42/44 MAPK), phospho-ERK (Y202/204), MEK, phospho-MEK (S217/221), mTOR, and cyclin D1 were purchased from Cell Signaling Tech, Danvers, MA.

The immunoreactive bands were visualized with a Super-Signal West Femto kit (Pierce). The scanned x-ray films were

---

[4] The abbreviations used are: Rb, retinoblastoma protein; hVSMC, human vascular smooth muscle primary cell(s); rRNA, ribosomal RNA; qPCR, quantitative PCR; mTOR, mammalian target of rapamycin; pol, polymerase; hCASMC, human coronary artery smooth muscle cells.

then analyzed with ImageJ software (National Institutes of Health) and Adobe PhotoShop.

*Data Analysis and Statistical Methods*—The comparative CT method (Applied Biosystems) was used to analyze the data resulting from the RT-qPCR experiments. Student's *t* test for unpaired results was performed to evaluate differences between two groups. Differences were considered to be significant for values of $p < 0.05$. All of the figures are assembled in FreeHand and Adobe PhotoShop.

## RESULTS

*Bilirubin Induces Growth Arrest in Proliferating Human Vascular Smooth Muscle Cells*—Vascular smooth muscle cell proliferation is known to be the key event in vascular response to injury. We examined the impact of bilirubin on cultured primary hVSMC from the coronary artery. Cellular proliferation was measured with the [$^3$H]thymidine incorporation assay. Cells cultivated with increasing concentrations of bilirubin exhibited lower thymidine incorporation (Fig. 1*A*, *lanes 3–5*), in a dose-dependent manner, than cells cultivated without bilirubin (*lane 2*). The lowest thymidine incorporation was observed in FBS-starved cells (*lane 1*).

To assess whether cellular apoptosis contributes to the observed low rate of thymidine incorporation, we performed an annexin V apoptosis assay. The results indicate that the same amounts of cells were undergoing apoptosis when cultivated in the presence or absence of bilirubin (Fig. 1*B*, *first lane*). Tested bilirubin concentrations up to 100 $\mu$M did not exhibit a significant increase in apoptosis. Less than 13% of the cells were stained positively for annexin V. In the positive control, significantly more cells were positively stained for annexin V in response to the apoptosis-inducing treatment with TNF$\alpha$ and IL-1$\beta$.

To further investigate the mechanism of the underlying bilirubin-induced inhibitory effect on cell proliferation, cell cycle analysis was performed with propidium iodine DNA staining and subsequent FACS analysis (Fig. 1*C*). The assay illustrated that the majority (>70%) of the cells that were cultured for 24 h in complete medium, FBS, and 100 $\mu$M bilirubin were growth arrested at the $G_0/G_1$ phase of the cell cycle. In the absence of bilirubin, however, significantly fewer cells (<60%) were found in the $G_0/G_1$ phase. In serum-starved cells, over 80% of the cells were found in the $G_0/G_1$ compartment of the cell cycle.

Thus, the sole mechanism by which bilirubin inhibits hVSMC proliferation is likely to be through growth arrest in the $G_0/G_1$ phase of the cell cycle. More importantly, the anti-proliferative effect is not due to cell death.

*Bilirubin Alters Rb Phosphorylation Pattern, Cellular YY1 Distribution, and Binding with Rb*—It is known that cell cycle transition from the $G_0/G_1$ to S phase is controlled by Rb phosphorylation (10). At least 16 different Rb amino acids are known to be differentially phosphorylated, which leads to altered Rb-protein transcription factor interactions and regulatory functions in gene transcription (11, 12). Therefore, we investigated whether bilirubin would change the amino acids phosphorylation profile of the cellular Rb. We performed Western blot experiments of total cell lysates from bilirubin-treated and untreated cells, with antibodies that recognize individual phos-
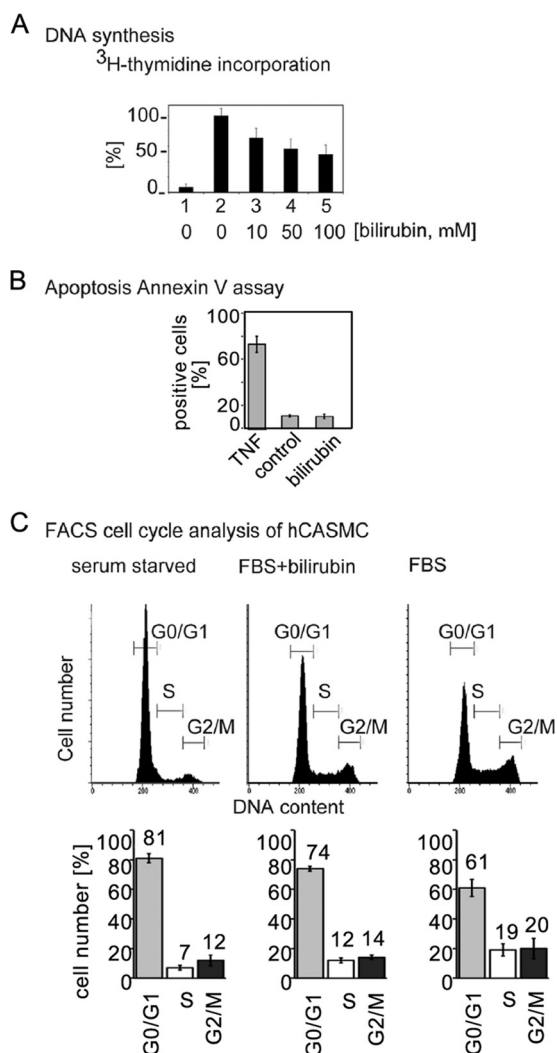


FIGURE 1. **Effect of bilirubin treatment on hVSMC proliferation and cell cycle transition.** Serum-starved hVSMC were cultivated in medium containing different concentrations of bilirubin and without bilirubin. *A*, [$^3$H]thymidine incorporation was measured for serum-starved cells (*lane 1*), FBS-stimulated cells (*lane 2*), and cells that are cultivated in medium with FBS and increasing concentrations of bilirubin: 10 $\mu$M (*lane 3*), 50 $\mu$M (*lane 4*), and 100 $\mu$M (*lane 5*) as indicated below the *bars*. The [$^3$H]thymidine content in cells that are cultivated in medium with FBS without bilirubin was used as reference (100%). *B*, annexin V apoptosis assay. Cells were cultivated with 100 $\mu$M bilirubin (*bilirubin*), without bilirubin (*control*), or with the proapoptotic mixture of TNF$\alpha$ (*TNF*, 400 units) and IL-1$\beta$ (100 units) as indicated below the *bars*. The number of apoptotic cells that stain positively for FITC-annexin V was determined by fluorescence microscopy. The total number of cells was taken as reference (100%). *C*, bilirubin treatment resulted in cellular growth arrest at the $G_0/G_1$ phase of the cell cycle as illustrated by the FACS profile. The cell cycle position of serum-starved cultures and cultivated cells with bilirubin and without bilirubin, as indicated above the profiles, was determined by propidium iodine staining of DNA and subsequent FACS analysis. Less than 1% of apoptotic cells were present in the cell cultures independently of the cell culture conditions. Each experiment is also illustrated by *diagrams* below the profiles where the *bars* present the quantity of cells in the $G_0/G_1$, S, and $G_2$ phases. The results from the experiments were obtained in triplicate. Three independent experiments produced consistent results. The values are the means S.E. (*n* = 3) in each group.

pho-Rb variants (Fig. 2). We observed hypophosphorylation of Rb at S780 (Fig. 2*A*) and S608 in cells cultivated in the presence of FBS and 100 $\mu$M bilirubin compared with cells cultivated in solely FBS-supplemented medium. These changes are consistent throughout 8, 16, and 24 h of bilirubin treatment. The hypophosphorylation pattern for S608 and S780 resembles the
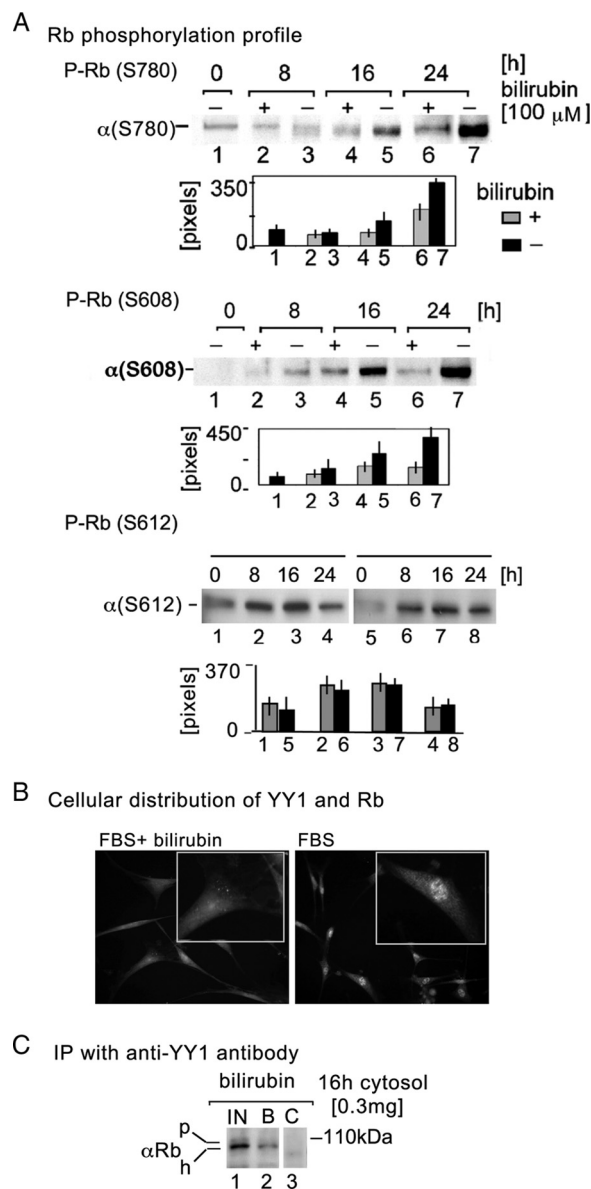
## A  Rb phosphorylation profile



**FIGURE 2. Bilirubin alters the Rb phosphorylation profile, YY1-Rb binding, and cellular YY1 localization.** Serum-starved hVSMC were cultivated in medium with 10% FBS and 100 $\mu$M bilirubin and compared for Rb phosphorylation profile and the presence of YY1-Rb complexes to cells that were cultivated without bilirubin. *A*, total cell lysates (100 $\mu$g of protein) were analyzed for content of phosphorylated Rb at Ser-780, Ser-612, and Ser-608 by Western blot with specific antibodies as indicated above the blots. *Lane 1*, Ser-608 and Ser-780 content in serum-deprived cells; *lane 2*, Ser-608 and Ser-780 content after 8 h of treatment with FBS and bilirubin (+); *lane 3*, 8 h of treatment with FBS alone (−); *lane 4*, 16 h of treatment with bilirubin; *lane 5*, 16 h of treatment with FBS alone (−); *lane 6*, 24 h of treatment with bilirubin (+); *lane 7*, 24 h of treatment minus bilirubin (−). The duration of treatment with FBS and bilirubin (+) and without bilirubin (−) is shown above the *lanes*. The Western blot results with anti-Rb (*S612*) antibody are presented as follows. *Lanes 1–4*, lysates from cells that are FBS-stimulated cells at different time points after stimulation as indicated above the *lanes*; *lanes 5–8*, FBS-stimulated cells together with bilirubin at different time points after stimulation. The intensity of the specific bands is measured in pixels as shown below the Western blot panels. The bilirubin (100 $\mu$M) presence (+, *gray bars*) or absence (−, *black bars*) is shown at the *right*. The values are the means ± S.E. of three independent experiments ($p < 0.05$ *versus* FBS-stimulated control). *B*, indirect immunofluorescent staining of cells with rabbit anti- Rb (Ser-612) (*red*) antibody and mouse anti-YY1 antibodies (*green*). The cells received FBS alone and together with bilirubin as indicated above the panels (original magnification, ×200; *insets* original magnification, ×400). FITC-labeled anti-mouse and Alexa 595-labeled anti rabbit antibodies were used for visualization by fluorescent microscopy. The co-localization of both proteins results in orange

serum-starved cells (Fig. 2*A*, *lane 1*). In contrary, the level of the phospho S612 variant does not change significantly in response to bilirubin. Hence, the variant serves as an internal control for equal protein loading.

The hypophosphorylated Rb binds YY1 and holds the protein in the cytosol (8). It is not known whether the Rb hypophosphorylation on S608 and S780 in bilirubin-treated cells will be sufficient to bind and prevent the YY1 migration to the nuclei. We verified the Rb-YY1 binding and cellular localization by immunofluorescence and antibodies to Rb (S612) and YY1. Following treatment with FBS together with bilirubin (Fig. 2*B*), most of the cells stained positively for the YY1-Rb complex in the cytosol (*orange*). In contrast, YY1 stained green in the nuclei of cells that received only FBS. In our second assay for the YY1-hypophosphorylated Rb binding in bilirubin-treated VSMC, we tested the ability of antibody to YY1 to capture the hypophosphorylated Rb (Fig. 2*C*). Consistent with the immunofluorescence results (Fig. 2*B*), YY1-specific antibody captured ~35% of the hypophosphorylated Rb (Fig. 2*C*, *lane 2*) in the cytosolic extract from 16-h bilirubin-treated cells (Fig. 2*C*, *lane 1*). Preimmune mouse antibody served as a negative control (Fig. 2*C*, *lane 3*).

Our experiments argue that treatment with 100 $\mu$M bilirubin in serum-stimulated hVSMC leads to hypophosphorylation of Rb at Ser-608 and Ser-780. The phosphorylation level at position Ser-612, however, remains high and is seemingly independent of the treatment. Importantly, the hypophosphorylated Rb variant in the bilirubin-treated cells is active to bind YY1 impeding the release to the nuclei.

*Bilirubin Has Effect on Raf/ERK/MAPK Pathway*—The Raf/MEK/ERK kinase pathway is a major pathway that has been shown to influence Rb phosphorylation, as well as cell cycle transitions. We assayed whether this pathway is influenced by treatment of hVSMC with bilirubin. Western blot experiments were performed with cell lysates from bilirubin-treated and untreated cells using antibodies that are specific to various total and phospho-forms of the kinases Raf, MEK1/2, and ERK1/2 proteins (Fig. 3). We observed that although total protein levels were constant, MEK1/2 and ERK1/2 were less phosphorylated 8 h after bilirubin treatment when compared with untreated cells (Fig. 3, *lanes 2* and *3*). The inhibitory effect of bilirubin on phosphorylation was most pronounced in ERK1/2 throughout the tested 24 h (Fig. 3, *lanes 1–7*). Bilirubin also showed an inhibitory effect on the cellular cyclin D1 level through the tested 24 h. In addition, less total Raf protein was detectable in the 24-h bilirubin fraction (*lanes 6*). The protein level of $\beta$-actin seems not to be altered by bilirubin treatment remaining nearly similar to the levels in the growth-arrested control cells before serum stimulation (Fig. 3, *lanes 2–7*). This protein serves as a control for equal protein loading.

staining. *C*, cytosol extract (0.3 mg) from 16-h bilirubin-treated cells were mixed and incubated with an affinity matrix containing covalently attached monoclonal antibody to YY1. Captured proteins were analyzed by Western blot with Rb-specific antibody. Samples are as follows: input lysate (*lane 1*, *IN*), bound and eluted by boiling in 1% SDS (*lane 2*, *B*), and captured with preimmune mouse antibody (*lane 3*, *C*). The apparent molecular mass (indicated to the *right* of the *panel*) of Rb was estimated by comparing the migration to protein size markers. The migration of the hyperphosphorylated (*p*) and the hypophosphorylated (*h*) Rb is shown on the *left*. *IP*, immunoprecipitation.
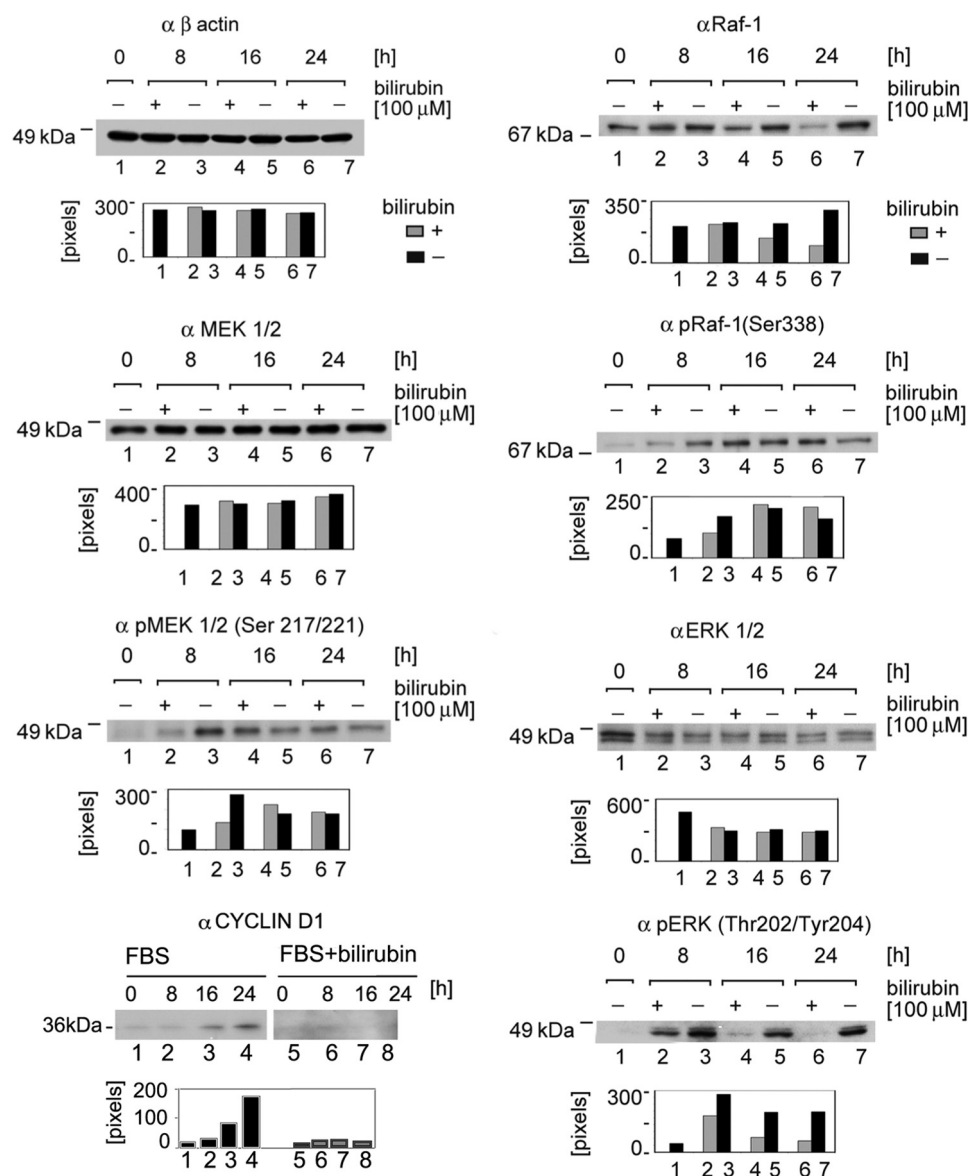
FIGURE 3. **Phosphorylation and total protein levels of Raf/ERK/MAPK pathway members in response to bilirubin.** Western blot analysis of total cell lysates from serum starved hVSMC (*lane 1*), cells treated with (+) and without (−) bilirubin for 8 h (*lanes 2* and *3*), 16 h (*lanes 4* and *5*), and 24 h (*lanes 6* and *7*). Protein-specific antibodies were used to monitor changes in protein content. Total *β*-actin protein content was used as a standard for equal protein loading, Raf protein content, phospho-Raf, total MEK1/2, phospho MEK1/2, ERK1/2, phospho-ERK1/2, and total cyclin D1. The identity of the specific antibodies is shown at the *top* of the panels. 40 *μ*g of protein is loaded in each of the lanes. Each experiment is also illustrated through *diagrams* below the panels in which the *bars* present the quantity (pixels) of immunologically reactive protein. The molecular mass of the proteins is shown at the *left* of the panels. The bilirubin (100 *μ*M) presence (+) or absence (−) in the cell cultures is shown above the *lanes* together with the duration (h) of treatment. The results are reproducible within three independent experiments. The *bars* present the average values of three independent experiments ($p < 0.05$ *versus* FBS-stimulated control).

The data argue for a specific inhibitory effect of bilirubin on Raf (S338), MEK (S217/221), and ERK (T202/Y204) phosphorylation. In addition, bilirubin-treated hVSMC have significantly less cyclin D1 protein, as well as Raf. The observed changes coincide with the bilirubin-specific profile of Rb hypophosphorylation (11) (Fig. 2) and cellular growth arrest (Fig. 1).

*Bilirubin Exposure Increases $Ca^{2+}$ Influx and Activation of Calpain II That Manifests in Proteolytical YY1 Cleavage*—Previously we reported that YY1 is a direct Rb target in VSMC (8). Hypophosphorylated Rb is known to restrain YY1 in the cytosol, preventing its migration into the nucleus to regulate genes that are directly involved in the hVSMC transition from growth arrest to the S phase (8). In Western blot experiments, we com-

pared the nuclear YY1 content in nuclear extracts from cell cultures after serum stimulation for 8 and 24 h in the presence or absence of bilirubin (Fig. 4A). The results consistently revealed the presence of >2 times less immunologically reactive full-length YY1 in bilirubin-treated cells (*lanes 3* and *5*) when compared with the serum-stimulated control cells (*lanes 2* and *4*).

The low YY1 protein content could reflect altered YY1 mRNA content in response to bilirubin treatment. Accordingly, we measured the YY1 mRNA content by RT-qPCR in bilirubin-treated and untreated cells. The YY1 mRNA content was found to remain relatively constant (Fig. 4B). Thus, the bilirubin-related alteration in YY1 protein content is likely to be

## A  Nuclear YY1 protein - western blot
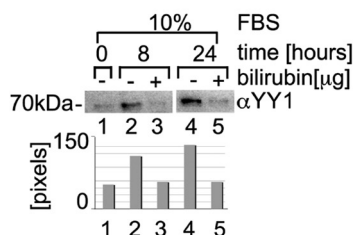


## B  RT-PCR
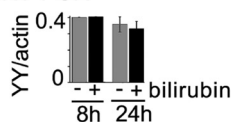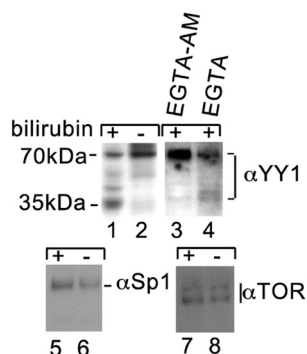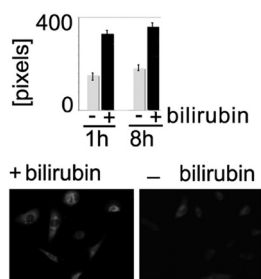


## C  Total Cell lysate-western blot



## D  Intracellular Ca content



FIGURE 4. **Ca²⁺ influx and proteolytic cleavage of YY1 in response to bilirubin treatment.** Bilirubin (100 $\mu$M) was added to the culture medium (+) together with FBS to stimulate growth. 8 and 24 h later, the cells were harvested for mRNA and protein analyses as indicated above the *lanes* and below the *bars*. Experiments with FBS alone without bilirubin were used as controls (−). *A*, nuclear cell lysates were used to determine the nuclear content of YY1 by Western blot. *B*, RT-PCR with YY1 gene-specific primers as indicated below the *bars*. Reactions with $\beta$-actin primers were used as an internal control. The *bars* represent fold changes in the presence of bilirubin ($p < 0.04$ *versus* FBS-stimulated cells). *C*, the cellular YY1, Sp1, and mTOR protein content is monitored in total cell lysates by Western blot with protein-specific antibody as indicated on the *right* of the panels. All of the reactions received equal amounts of protein (50 $\mu$g). *Lane 1*, total cell lysate from cells after 24 h of treatment with bilirubin; *lane 2*, cells in the absence of bilirubin; *lane 3*, cell lysate from cells that are grown in the presence of bilirubin and EGTA-AM (*AM*); *lanes 4*, cells are grown in the presence of bilirubin and EGTA; *lane 5* and *6*, Sp1-specific antibody identifies the presence of Sp1 protein in the lysates; *lane 7* and *8*, mTOR-specific antibody identifies the presence of total mTOR protein. The YY1, Sp1, and mTOR antibodies reactive bands are indicated on the *right*. The size markers migration is shown on the *left* (kDa). The results are consistent between two independent experiments. *D*, cells were serum-stimulated without (−) and with (+) bilirubin (100 $\mu$M). 1 and 8 h later, the cells were treated with the Ca²⁺ indicator fura red for 20 min, and the intracellular Ca²⁺ content is shown by fluorescent microscopy at 550-nm excitation. *Red* corresponds to the intracellular fura red-Ca²⁺ complex. The *red color*

post-translationally regulated. To assay for degradation of the protein upon bilirubin treatment, we performed Western blots with polyclonal anti-YY1 antibodies (Fig. 4*C*) and total cell extract. The blots indicate the presence of faster migrating YY1 ~35-kDa fragments (13) in the bilirubin cell culture lysates, suggesting an intracellular proteolysis of YY1 (Fig. 4*C, lane 1*). The cleavage is YY1-specific because two other assayed zinc finger transcription factors, Sp1 and mTOR, remain intact (Fig. 4*C, lanes 5–8*). The proteolytic YY1 cleavage is likely to be caused by the activation of the Ca²⁺-dependent protease calpain II, which cleaves YY1 in other cell types (13). We carried out 8-h bilirubin treatment in the presence of the potent membrane-permeable calcium chelator EGTA-AM and EGTA that does not enter the cells. We observed that YY1 cleavage was diminished when the EGTA-AM was added to the medium (Fig. 4*C, lane 3*). The extracellular Ca²⁺ chelator EGTA, however, has little effect on reducing the suggested calpain II-YY1 cleavage (Fig. 4*C, lane 4*) (14).

Changes in the intracellular Ca²⁺ content in response to bilirubin could activate calpain II and potentially account for the observed YY1 cleavage. We measured and compared the intracellular Ca²⁺ level in serum-stimulated cells that are cultivated in the presence of 100 $\mu$M bilirubin (Fig. 4*D*) for 1 and 8 h. The data clearly demonstrate that 1 h of treatment with bilirubin results in more than two times Ca²⁺ level elevation when compared with the control cells. The Ca²⁺ level remains high 8 h after adding bilirubin to the cell culture medium.

Collectively, our data document the ability of bilirubin to alter the Ca²⁺ influx and possibly induce the activation of the Ca²⁺-calpain II circuit in hCASMC. We suggest that these cellular events ultimately manifest in the cleavage of YY1.

*Altered Expression of RNA Polymerase I, Polymerase II, and Polymerase III Transcribed Genes in Response to Bilirubin*—We observed alterations in cell growth, the Raf/ERK/MAP kinase pathway, and the pattern of Rb phosphorylation, together with the reduced cellular YY1 content in bilirubin-treated cells. This could result in altered transcription of genes with cell cycle transition functions that are known to be regulated by YY1 and Rb-YY1 interaction. YY1 participates in the regulation of all three DNA-dependent RNA polymerases, RNA polymerase (pol) I, pol II, and pol III (15–18). It is also known that ribosome biogenesis is tightly regulated during the cell cycle and differentiation processes (19). We thus tested whether cells treated with bilirubin exhibit an altered transcript levels of 45 S rRNA and 5 S rRNA (Fig. 5) by RT-qPCR analysis. The 45 S rRNA that is transcribed by pol I does not decrease within the initial 8 h of treatment. However, a decrease is observed 16 and 24 h after adding bilirubin to the growth medium. The pol III transcribed 5 S rRNA significantly decreased earlier after the first 8 h. Importantly, bilirubin treatment coincides with a time-dependent elevation in mRNA content of the pol II transcribed VSMC differentiation marker, the smooth muscle $\alpha$-actin.

intensity in the cells is measured in pixels. The measurements were performed in triplicate. Three independent experiments produced consistent results ($p < 0.03$). A fluorescent microscopy picture of bilirubin-treated (+) and control (−) cells (8 h) is shown below the *bars*.
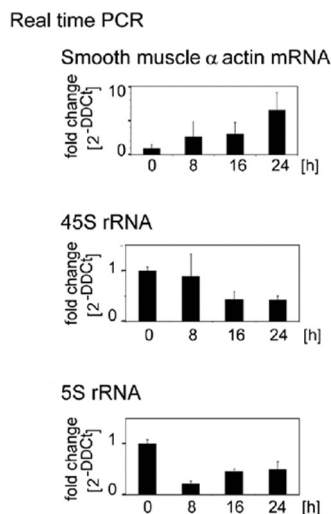
Real time PCR

Smooth muscle α actin mRNA



45S rRNA



5S rRNA



FIGURE 5. **Effect of bilirubin on pol I, pol II, and pol III transcribed RNAs in hVSMC.** Total RNA was isolated from bilirubin-treated and untreated cell cultures and used in RT-qPCRs with gene-specific primers for: pol II transcribed smooth muscle actin, 45 S rRNA transcribed by pol I, and 5 S rRNA transcribed by pol III as indicated above the *diagrams*. The *bars* represent the fold change in specific RNA content using the *β*-actin mRNA level as an endogenous reference gene that does not change in response to treatment. PCRs were conducted with total RNAs isolated from cell cultures after 0, 8, 16, and 24 h of bilirubin treatment as indicated below the *bars*. Three independent experiments produced consistent results (S.D. ± ~3%).

This suggests that bilirubin could arrest hVSMC cell growth by inhibiting the expression of pol I- and pol III-transcribed 5 S rRNA and 45 S rRNA. Although the rRNAs content goes down, bilirubin has a positive effect on the mRNA content of the pol II transcribed marker of VSMC differentiation, the smooth muscle $α$-actin, which is known to be repressed by YY1 (8).

## DISCUSSION

There is considerable clinical evidence that elevated serum bilirubin levels are associated with a diminished susceptibility to atherosclerotic vascular disease (5–7). However, these findings do not necessarily implicate bilirubin as the protective agent at the cellular level. Because vascular smooth muscle cell proliferation is a key event in the vascular response to injury and bilirubin is known to inhibit the development of atherosclerotic vascular disease, we examined the impact of bilirubin on hVSMC proliferation in primary human cell cultures. Treating the cells with bilirubin inhibited the cell proliferation in a dose-dependent manner, whereas extensive proliferation was found in the control cells (no bilirubin). In addition, although FBS-stimulated control cells began to progress throughout the cell cycle upon serum starvation, as seen by FACS analysis, the bilirubin treatment retained the cells in the $G_0/G_1$ arrest. More importantly, the hVSMC response to bilirubin at the tested high physiological concentration does not cause apoptosis as shown by annexin V staining. This absence of apoptosis is significant given recent reports that apoptosis of VSMCs can trigger the development of neointima formation (20).

Our data suggest that at certain concentrations bilirubin triggers a nontoxic cascade of molecular events that block hVSMC proliferation. Bilirubin clearly alters the phosphorylation status of Rb, a protein with crucial $G_1/S$ checkpoint functions that are essential for the cell cycle transitions (10). The bilirubin treatment coincides with specific dephosphorylation of Rb at Ser-780 and Ser-608 while preserving the phospho S612. Such a profile of Rb phosphorylation is likely to be essential for keeping the hVSMC in a growth-arrested state. Importantly, it facilitates Rb interactions with specific transcription factors, including YY1 (8) and its cytoplasmic retention with direct consequences on gene transcription (8).

One of the major cell signaling pathways known to alter the phosphorylation status of Rb at S780 and S608 is the Raf/ERK/MAPK pathway (21). We observed that a significant portion of ERK1/2 is hypophosphorylated in bilirubin-treated cells. Similarly, Raf and MEK are also hypophosphorylated, albeit to a lesser extent. It remains unclear how bilirubin promotes the accumulation of the nonphosphorylated protein forms. Bilirubin could, for example, inhibit Raf phosphorylation by inhibiting pathways upstream of Ras in a smooth muscle cell-specific manner (22). It is known that Ras directly interacts with and activates Raf by phosphorylation. Raf next phosphorylates and activates MEK, which in turn phosphorylates and activates ERKs. Therefore, the observed low cellular Raf protein content and hypophosphorylation in response to bilirubin could trigger low levels of MEK and ERK phosphorylation and pathway inactivation. Through Raf, bilirubin could also act in a cascade-independent fashion, for example by inactivating transcription factor NF-κB. Such a scenario could explain, at least in part, the lower level of apoptosis in bilirubin-treated hVSMC. Taillé *et al.* (23) suggested that bilirubin in airway smooth muscle cells could also modulate the phosphorylation of ERK by a redox mechanism. Furthermore, bilirubin could also modulate other cell signaling pathways that are cross-talking with the ERK/MAPK pathway. The p38 pathway, for instance, could interact with the ERK pathway to alter phosphorylation of up- and downstream proteins. Such a hypothesis is supported by our previous observation that bilirubin treatment coincides with accumulation of underphosphorylated p38, a major kinase in the MAPK signaling pathway in mouse and rat SMCs (8).

The observation that the cellular cyclin D1 protein content is highly reduced in response to bilirubin treatment is significant. Cyclin D1 is one of the major cellular cyclins in terms of its functional importance for the cell cycle transitions. The cyclin D-Cdk4/6 complex partially phosphorylates Rb to trigger S phase progression (24). The observed low level of cyclin D1 together with the accumulation of underphosphorylated ERK could explain the appearance of hypophosphorylated Rb and the growth arrest in the bilirubin-treated cell cultures.

The effect of bilirubin on cell signaling pathways is most likely a complex event including redox and other mechanisms that control the cell cycle status. The exact mechanisms that control the low cellular Raf and cyclin D1 levels in response to bilirubin, however, are important and remain to be determined.

Bilirubin treatment coincides with a reduced YY1 protein level. In this study, we did not witness changes in YY1 mRNA levels. The lower YY1 protein content is a result of a bilirubin-triggered specific YY1 proteolytic cleavage. No proteolysis of other zinc finger transcription factors including Sp1 and mTOR could be observed. The increase in YY1-specific cleavage is likely to be a consequence of activated calcium influx and calpain II protease activation. Supporting evidence corroborat-
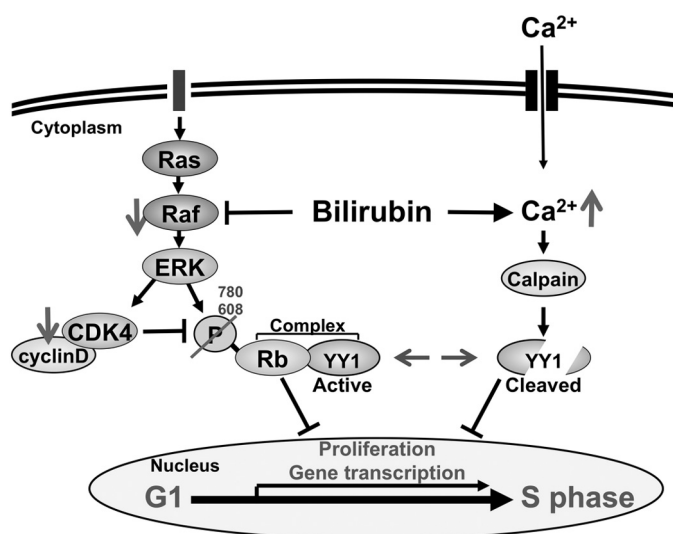
FIGURE 6. **Model of the molecular mechanism of bilirubin-induced growth arrest in hVSMC.** Bilirubin treatment decreases the cellular protein content of cyclin D1 and Raf. It also inhibits phosphorylation and activation of members of the Raf/ERK/MAPK pathway, resulting in the accumulation of hypophosphorylated at Ser-608 and Ser-780 Rb that is a key suppressor of cell cycle transition from $G_0/G_1$ into S phase. The hypophosphorylation profile of Rb facilitates Rb-YY1 binding, retention in the cytosol, and consequent nuclear YY1 depletion. Bilirubin also activates intracellular $Ca^{2+}$ influx, $Ca^{2+}$-calpain protease circuit activation, and YY1 cleavage, further altering the nuclear YY1 availability for transcription. The reduced level of nuclear YY1 results in altered mRNA content of pol I, pol II, and pol III transcribed genes with important functions in the VSMC cell cycle control.

ing the idea that bilirubin could have an effect on the calcium influx, on calpain II activation in hVSMC, and YY1 degradation, was previously reported for neuronal cell cultures (3). Cleavage of YY1 by calpain II is likely to play important regulatory functions in the myogenic differentiation (13). The calcium influx activation together with the involvement of YY1 cleavage mechanism in the hVSMC growth arrest response to bilirubin is novel. Targeting proteases to a transcriptional machinery may represent a unique feature in the vascular gene regulation and the response to injury.

Bilirubin significantly inhibited the expression of the pol I and pol III transcribed 45 S rRNA and 5 S rRNAs. The availability of these RNAs ultimately determines the ribosomal assembly and the cellular potential for growth and proliferation (15, 16). Because YY1 and Rb are both implicated in the regulation of pol I and pol III transcribed genes (17, 18), changes in the status of Rb phosphorylation together with the decreased protein level of YY1 most likely underlie the reduced 45 S and 5 S rRNA level of expression. It is possible that the bilirubin-related Rb profile of amino acids hypophosphorylation retains YY1 in the cytosol, forming a Rb-YY1 complex that prevents YY1 migration to the nuclei and subsequent activation of 5 S and 45 S rRNA transcription. Such a notion is directly supported by our previous data showing that a direct correlation exists between levels of cellular hypophosphorylated Rb, cytosolic Rb-YY1 content, and the hCASMC cell cycle phase (8). In addition, proteolytic cleavage also contributes to the functional nuclear YY1 deficiency, as shown in this study.

Taken together, our data suggest that bilirubin treatment inhibits hVSMC growth through two mechanisms. First, the impaired activation of Raf/ERK/MAPKs together with the reduced content of cellular cyclin D1 and Raf proteins results in inhibited Rb phosphorylation on serines S608 and S780. These events impede the release of transcription factors that are important for VSMC growth, such as YY1. Second, there is an increase in specific YY1 protein cleavage as a result of possible bilirubin-related change in the calcium influx and calpain II protease activation. The reduced cellular protein level of the transcription factor YY1 itself results in a suppressed capacity to induce ribosomal RNA synthesis and cell proliferation (Fig. 6).

Our observations suggest that at high normal levels, bilirubin does not cause human VSMC cell death. As we have shown in this study, there are candidate molecules and pathways that could explain the association of high normal bilirubin levels and the maintenance of human vascular homeostasis. These observations provide new mechanistic insights into the molecular players and pathways underlying the transition of hVSMC from proliferative to contractile phenotype and the response to bilirubin. They may provide opportunities for the development of novel therapeutic strategies to target vascular response to injury and neointimal formations.

## REFERENCES

1. Mustafa, M. G., Cowger, M. L., and King, T. E. (1969) Effects of bilirubin on mitochondrial reactions. *J. Biol. Chem.* **244,** 6403–6414
2. Hahm, J. S., Sung, I. K., Yang, S. C., Rhee, J. C., Lee, M. H., Kee, C. S., and Park, K. N. (1992) Biliary proteins in patients with and without gallstones. *Korean J. Intern Med.* **7,** 18–24
3. Grojean, S., Koziel, V., Vert, P., and Daval, J. L. (2000) Bilirubin induces apoptosis via activation of NMDA receptors in developing rat brain neurons. *Exp. Neurol.* **166,** 334–341
4. Stocker, R., Yamamoto, Y., McDonagh, A. F., Glazer, A. N., and Ames, B. N. (1987) Bilirubin is an antioxidant of possible physiological importance. *Science* **235,** 1043–1046
5. Perlstein, T. S., Pande, R. L., Beckman, J. A., and Creager, M. A. (2008) Serum total bilirubin level and prevalent lower-extremity peripheral arterial disease: National Health and Nutrition Examination Survey (NHANES) 1999 to 2004. *Arterioscler. Thromb. Vasc. Biol.* **28,** 166–172
6. Troughton, J. A., Woodside, J. V., Young, I. S., Arveiler, D., Amouyel, P., Ferrières, J., Ducimetière, P., Patterson, C. C., Kee, F., Yarnell, J. W., Evans, A., and PRIME Study Group (2007) Bilirubin and coronary heart disease risk in the Prospective Epidemiological Study of Myocardial Infarction (PRIME). *Eur. J. Cardiovasc Prev. Rehabil.* **14,** 79–84
7. Vítek, L., Jirsa, M., Brodanová, M., Kalab, M., Marecek, Z., Danzig, V., Novotný, L., and Kotal, P. (2002) Gilbert syndrome and ischemic heart disease. A protective effect of elevated bilirubin levels. *Atherosclerosis* **160,** 449–456
8. Petkova, V., Romanowski, M. J., Sulijoadikusumo, I., Rohne, D., Kang, P., Shenk, T., and Usheva, A. (2001) Interaction between YY1 and the retinoblastoma protein. Regulation of cell cycle progression in differentiated cells. *J. Biol. Chem.* **276,** 7932–7936
9. Ollinger, R., Bilban, M., Erat, A., Froio, A., McDaid, J., Tyagi, S., Csizmadia, E., Graça-Souza, A. V., Liloia, A., Soares, M. P., Otterbein, L. E., Usheva, A., Yamashita, K., and Bach, F. H. (2005) Bilirubin. A natural inhibitor of vascular smooth muscle cell proliferation. *Circulation* **112,** 1030–1039
10. Chau, B. N., and Wang, J. Y. (2003) Coordinated regulation of life and death by RB. *Nat. Rev. Cancer* **3,** 130–138
11. Sherr, C. J. (1994) $G_1$ phase progression. Cycling on cue. *Cell* **79,** 551–555
12. Zhu, L. (2005) Tumour suppressor retinoblastoma protein Rb. A transcriptional regulator. *Eur. J. Cancer* **41,** 2415–2427
13. Walowitz, J. L., Bradley, M. E., Chen, S., and Lee, T. (1998) Proteolytic regulation of the zinc finger transcription factor YY1, a repressor of mus-

cle-restricted gene expression. *J. Biol. Chem.* **273,** 6656 – 6661

14. Sen, C. K., Roy, S., and Packer, L. (1996) Involvement of intracellular Ca$^{2+}$ in oxidant-induced NF-$\kappa$B activation. *FEBS Lett.* **385,** 58 – 62

15. Grummt, I. (2003) Life on a planet of its own. Regulation of RNA polymerase I transcription in the nucleolus. *Genes Dev.* **17,** 1691–1702

16. Moss, T., and Stefanovsky, V. Y. (2002) At the center of eukaryotic life. *Cell* **109,** 545–548

17. Felton-Edkins, Z. A., Kenneth, N. S., Brown, T. R., Daly, N. L., Gomez-Roman, N., Grandori, C., Eisenman, R. N., and White, R. J. (2003) Direct regulation of RNA polymerase III transcription by RB, p53 and c-Myc. *Cell Cycle* **2,** 181–184

18. Kurose, K., Hata, K., Hattori, M., and Sakaki, Y. (1995) RNA polymerase III dependence of the human L1 promoter and possible participation of the RNA polymerase II factor YY1 in the RNA polymerase III transcription system. *Nucleic Acids Res.* **23,** 3704 – 3709

19. Leicht, D. T., Balan, V., Kaplun, A., Singh-Gupta, V., Kaplun, L., Dobson, M., and Tzivion, G. (2007) Raf kinases. Function, regulation and role in human cancer. *Biochim. Biophys. Acta* **1773,** 1196 –1212

20. Beohar, N., Flaherty, J. D., Davidson, C. J., Maynard, R. C., Robbins, J. D., Shah, A. P., Choi, J. W., MacDonald, L. A., Jorgensen, J. P., Pinto, J. V., Chandra, S., Klaus, H. M., Wang, N. C., Harris, K. R., Decker, R., and Bonow, R. O. (2004) Antirestenotic effects of a locally delivered caspase inhibitor in a balloon injury model. *Circulation* **109,** 108 –113

21. Garnovskaya, M. N., Mukhin, Y. V., Vlasova, T. M., Grewal, J. S., Ullian, M. E., Tholanikunnel, B. G., and Raymond, J. R. (2004) Mitogen-induced rapid phosphorylation of serine 795 of the retinoblastoma gene product in vascular smooth muscle cells involves ERK activation. *J. Biol. Chem.* **279,** 24899 –24905

22. Dumaz, N., and Marais, R. (2005) Raf phosphorylation one step forward and two steps back. *Mol. Cell.* **17,** 164 –166

23. Taillé, C., Almolki, A., Benhamed, M., Zedda, C., Mégret, J., Berger, P., Lesèche, G., Fadel, E., Yamaguchi, T., Marthan, R., Aubier, M., and Boczkowski, J. (2003) Heme oxygenase inhibits human airway smooth muscle proliferation via a bilirubin-dependent modulation of ERK1/2 phosphorylation. *J. Biol. Chem.* **278,** 27160 –27168

24. Musgrove, E. A., Caldon, C. E., Barraclough, J., Stone, A., and Sutherland, R. L. (2011) Cyclin D as a therapeutic target in cancer. *Nat. Rev. Cancer* **11,** 558 –572